DOI: 10.1111/j.1467-8659.2009.01638.x

EUROGRAPHICS 2010 / T. Akenine-Möller and M. Zwicker
(Guest Editors)

Volume 29 (2010), Number 2

A Hybrid Approach to Multiple Fluid Simulation using Volume Fractions

Nahyup Kang[1†] Jinho Park[2] Junyong Noh[1] Sung Yong Shin[1]

[1]Korea Advanced Institute of Science and Technology
[2]Namseoul University

Abstract

This paper presents a hybrid approach to multiple fluid simulation that can handle miscible and immiscible fluids, simultaneously. We combine distance functions and volume fractions to capture not only the discontinuous interface between immiscible fluids but also the smooth transition between miscible fluids. Our approach consists of four steps: velocity field computation, volume fraction advection, miscible fluid diffusion, and visualization. By providing a combining scheme between volume fractions and level set functions, we are able to take advantages of both representation schemes of fluids. From the system point of view, our work is the first approach to Eulerian grid-based multiple fluid simulation including both miscible and immiscible fluids. From the technical point of view, our approach addresses the issues arising from variable density and viscosity together with material diffusion. We show that the effectiveness of our approach to handle multiple miscible and immiscible fluids through experiments.

Categories and Subject Descriptors (according to ACM CCS): I.3.7 [Computer Graphics]: Computer Graphics—Three-Dimensional Graphics and Realism

1. Introduction

Multiple fluid phenomena involving both miscible and immiscible fluids are often observed in our life, for example, pouring milk into coffee, dropping ink into water, making cocktail drinks, to name a few. In each of the examples, a pair of fluids is mixed smoothly while creating the sharp interface with air. Complicated fluid phenomena involve more diverse combinations of miscible and immiscible fluids. Recently, multi-fluid simulation has drawn much attention. However, simulating such phenomena is still difficult although partial solutions have been reported [GDSS05, MSKG05, LSSF06, ZLLW06, ZBWL07, PKW*08].

We propose a hybrid simulation method for simulating miscible and immiscible fluids simultaneously by combining distance functions(level set functions) [OS88, LSSF06] and volume fractions [HN81, GDSS05]. Our approach effectively handles the discontinuous interface between immiscible fluids and smooth transition of miscible fluids, while adopting the standard operator-splitting framework [Sta99] to solve the Navier-Stokes equations on a MAC grid [HW65].

In our problem setting, fluids of various densities and viscosities move around in the simulation space. These fluids are classified into groups of fluids according to their miscibilities. Each group represents a mixture of miscible fluids and is immiscible with the others. In order to keep track of the spatial distribution of each fluid at every time step, we represent the fluid mix in a grid cell by a vector of volume fractions, where each volume fraction gives the percentage of the cell volume occupied by the corresponding fluid. Although multiple fluids can be handled effectively exploiting volume fractions regardless of their miscibility, it is difficult to directly identify the interface between immiscible fluids from the volume fractions due to their non-geometric nature. Therefore, we modify the volume fractions of cells near the interface at every time step using a fast marching method in order to track the interface between immiscible fluids with the volume fractions. Based on this modification, we can

† nhkang@jupiter.kaist.ac.kr

take advantages of both volume fractions and level set functions.

Given the volume fractions, the aggregate density of the fluids in a cell is the sum of their individual densities weighted by the corresponding volume fractions. The aggregate viscosity can also be computed in the same manner. As both quantities vary spatially, we have to solve Navier-Stokes equations with variable density and viscosity while capturing the discontinuity and the continuity of these quantities.

Provided with a flow field, yet another issue is how to advect the volume fractions while minimizing their numerical dissipation. Although a VOF method [HN81] conserves the volumes of fluids during their advection, we cannot use this method after the modification of volume fractions since the sum of volume fractions of a cell near the interface is not equal to one any more. Our solution first advects the volume fraction of each fluid using the back and forth error compensation and correction(BFECC) scheme [KLLR07]. For accurate tracking of the interface, the level set functions are also extracted from the modified volume fractions of cells. Then an existing particle level set method [EFFM02, EMF02, ELF05, LSSF06] is employed for correcting these functions. The corrected level set functions are converted back to the volume fractions near the interface.

Finally, given the volume fractions at each grid cell, we address the material diffusion issue for miscible fluids. We adopt an additional diffusion equation to model the material diffusion of miscible fluids since Navier-Stokes equations do not have an inherent capability of dealing with material diffusion. The discontinuous interface between immiscible fluids as well as continuous transition of miscible fluids is visualized using the finally-obtained volume fractions.

The contributions of our paper can be summarized as follows: From the system point of view, our work is the first approach to Eulerian grid-based multiple fluid simulation including both miscible and immiscible fluids. From the technical point of view, our contributions are three-fold:

- We show that the divergence-free condition in incompressible Navier-Stokes equations can be satisfied in our problem setting even with miscible fluids(variable density) under a reasonable assumption(Section 3.2). We also show that an existing solver for viscosity integration [LSSF06, BB08] can be employed for variable viscosity integration under the same assumption(Section 4.2).

- We present a hybrid scheme by combining volume fractions and level set functions in order to handle both the discontinuous interface between immiscible fluids and the smooth transition between miscible ones(Section 5).Specifically, this scheme can simulate the interaction between the immiscible fluids while simultaneously taking care of the diffusion between miscible fluids, which are hard to grasp with existing methods [ZLLW06, ZBWL07, MMTD07, PKW*08] because of spatially varying fluid densities and viscosities.

- We propose a stable material diffusion method which allows diffusions only between miscible fluids. The material diffusion equation is simplified by modelling diffusion phenomena based on volume fractions rather than mass fractions(Section 6 and Appendix B).

The remainder of the paper is organized as follows: The next section reviews previous work. Section 3 provides our key results: volume fraction representation of fluids, incompressibility condition enforcement, and combination of volume fractions and distance functions. In Section 4 we describe how to compute a divergence-free velocity field for a fluid flow with both density and viscosity varying spatially. Section 5 and 6 deal with volume fraction advection and miscible fluid diffusion, respectively. We briefly discuss fluid visualization in Section 7. Section 8 shows experimental results. We conclude the paper in Section 10.

2. Related Work

Multiple Fluid Interactions: Due to recent advancement of fluid simulation technology, multiple fluid interactions have drawn much attention from the computer animation community: Premože et al. presented a particle-based method which can simulate multiple immiscible fluids [PTB*03]. Müller et al. [MSKG05] proposed a smoothed particle hydrodynamics(SPH)-based method [Mon05, MCG03] for modeling fluid-fluid interaction. Hong et al. [HK05] simulated incompressible viscous two-phase fluids with realistic small-scale details using ghost fluid methods [LFK00, KFL00]. Losasso et al. [LSSF06] simulated multiple immiscible fluids by extending particle level set(PLS) methods [EFFM02, EMF02, ELF05] on an Eulerian grid. These particle level set methods cannot be extended to multiple miscible fluid simulation since the methods assume that the density is constant inside the fluid. However, for the accurate tracking of the volume fractions near the interface between immiscible fluids, we exploit the particle-based level set method by Losasso et al. [LSSF06].

Zhu et al. [ZLLW06, ZBWL07] simulated a pair of miscible fluids based on a Lattice Boltzmann Method(LBM) [CD98]. LBM-based approaches suffer from instability that tends to produce high-Reynold number effects, resulting in viscous-looking fluid flows. Moreover, an LBM-based method cannot deal with the divergence-free condition of fluids. We employ the operator-splitting framework [Sta99] for solving Navier-Stokes equations in order to satisfy the divergence-free condition for multiple fluids regardless of their miscibility. Recently, Mullen et al. [MMTD07] proposed a mass-preserving density advection method that can handle miscible fluids. However, this method did not take into account

variable densities and viscosities. Moreover, it is not obvious how to extend the method to handle both multiple miscible and immiscible fluids.

Park et al. [PKW*08] presented an LBM-based approach to simulate more complex phenomena involving both immiscible and miscible fluids based on a phase field method(PFM) [AMW98]. This approach suffers from several limitations such as volume loss, large memory requirements, and viscous-looking flow generation. Moreover, the governing equations of the PFM include a 4^{th} order differential term, which makes it difficult to solve them numerically and tends to smooth out the interface so as to make small drops shrink spontaneously [YZF07].

Volume-of-Fluid based Methods: Volume-of-Fluid(VOF) methods [HN81] have also been used widely as alternatives for tracking fluids on an Eulerian grid. A VOF method does not track the motion of the interface between fluids, but evolves the volume fraction of each material. The interface between fluids is reconstructed from the volume fractions by employing an approximation method such as piecewise linear interface calculation(PLIC) scheme [You82]. The main advantage of the VOF method is that it can conserve fluid volumes explicitly by computing volume fluxes. However, the reconstruction of the material interface while satisfying volume constraints over a spatial domain is a difficult problem because of its under-constrained nature. The PLIC scheme also suffers from several limitations such as discontinuity across the cell boundaries and ambiguity for three or more materials. Several variations of the PLIC scheme have been presented to resolve those limitations [PP04, GDSS05, AGDJ08]. Yet another limitation lies in difficulty of computing interfacial normals and curvatures that are important to solve Navier-Stokes equations, in particular, computing surface tension forces.

Sussman et al. presented a hybrid approach by coupling a level set method and a VOF method(CLSVOF) [SP00, Sus03, MUM*06] for accurate interfacial curvature calculation and mass conservation. In the CLSVOF method, a PLIC scheme reconstructs the interface between fluids from the volume fractions. Then, the interface is used to correct(redistance) a level set function from which an interfacial curvature is computed. However, it is not easy to extend the CLSVOF method to tracking multiple fluids since both interface reconstruction and level set correction are complicated even in a two-phase flow. Detailed comparison between particle level set methods and CLSVOF methods is well discussed in [WYS08, GA08].

We adopt volume fractions as the base representation scheme for multiple fluids regardless of their miscibilities. We modify the volume fractions near the interface to represent a distance function as well, in order to capture both the interface between immiscible fluids and the smooth transition between miscible fluids(See Section 3.3). Based on this representation scheme, we make use of a particle level set method for tracking the interface between multiple immiscible fluids [LSSF06] while correctly diffusing the volume fractions between miscible fluids.

3. Multiple Fluid Flow

We employ following Navier-Stokes equations to simulate incompressible fluids with variable viscosity:

$$\mathbf{u}_t = -(\mathbf{u}\cdot\nabla)\mathbf{u} - \frac{1}{\rho}\nabla p + \frac{1}{\rho}\nabla\cdot\tau + \mathbf{f}, \tag{1}$$

$$\nabla\cdot\mathbf{u} = 0, \tag{2}$$

$$\tau = \mu(\nabla\mathbf{u} + (\nabla\mathbf{u})^T), \tag{3}$$

where $\mathbf{u}$ is velocity, μ is viscosity, p is pressure, ρ is density, τ is the viscous shear stress tensor, and $\mathbf{f}$ represents body forces such as gravity and surface tension. We note that the density and viscosity of the fluid mixture vary spatially because of miscible fluids. At first glance, it appears that the incompressibility condition(Equation (2)) would not be satisfied, and thus the above equations may not be suitable for our problem.

In this section, we set up the cornerstones of our approach. We first introduce a multiple fluid representation scheme based on volume fractions. We then show that the incompressibility condition is satisfied under a practical assumption, so as to adopt the Navier-Stokes equations for our purpose regardless of the miscibilities of participating fluids. We finally describe how to combine volume fractions and signed distance functions.

3.1. Multiple Fluid Representation

We describe how to represent multiple fluids including both immiscible and miscible ones using their volume fractions.

Volume Fractions: Let V and V^f be the volume of a cell and the portion of the cell volume occupied by fluid f, respectively. The volume fraction of fluid f, denoted by α^f, is said to be the ratio of V^f to V. $\alpha^f = V^f/V = V^f/\sum_f V^f$.

Suppose that N fluids are involved in simulation. Then, their volume fractions can be represented as a vector, $(\alpha^{f_1}, \alpha^{f_2}, \cdots, \alpha^{f_N})$. Notice that our simulation is done on a regular grid, and thus all grid cells have the same volume V. Since the mass of the aggregate fluid in a cell i is $M_i = \rho_i V = \sum_f \alpha_i^f \rho_i^f V$, the density of the aggregate fluid(or fluid mixture) in the cell is $\rho_i = \sum_f \alpha_i^f \rho_i^f$.

Groups of miscible fluids: In order to represent a multiple fluid flow, we classify the fluids into groups such that only the fluids in the same group are miscible. For example, a set of four different fluids, {air, water, ink, oil} are classified into three groups {air}, {water, ink}, and {oil}. Here,

only one pair of fluids, water and ink are miscible with each other. A group in a cell is said to be dominant if the sum of the volume fractions of the group is larger than those of the others.

3.2. Incompressibility Condition

In computer graphics, the conservation of mass equation(Equation (2)) is commonly used under a constant density assumption. Since the density of fluids varies spatially because of miscible fluids, we have to show that this equation does still hold true. Otherwise, we would not use the operator-splitting scheme [Sta99] for solving Navier-Stokes equations. Most previous work [ZLLW06, ZBWL07, PKW*08] ignored the divergence-free condition for multiple miscible fluids.

To show that divergence-free condition still holds even for multiple miscible and immiscible fluids, we start with a general continuity equation with possibly variable density ρ.

$$\frac{\partial \rho}{\partial t} + \nabla \cdot (\rho \mathbf{u}) = 0. \tag{4}$$

We assume that individual density ρ^f is constant for all fluid f. This assumption means that even if fluid f is mixed with other fluids, its volume does not change. Integrating Equation (4) over a cell for each fluid f and applying the divergence theorem to the result, we derive

$$\frac{\partial \alpha^f \rho^f}{\partial t} + \nabla \cdot \left(\alpha^f \rho^f \mathbf{u} \right) = 0. \tag{5}$$

Since ρ^f is constant, Equation (5) can be reduced to

$$\frac{\partial \alpha^f}{\partial t} + \nabla \cdot \left(\alpha^f \mathbf{u} \right) = 0. \tag{6}$$

Adding Equation (6) for all f, we obtain

$$\frac{\partial \sum \alpha^f}{\partial t} + \nabla \cdot \left(\left(\sum \alpha^f \right) \mathbf{u} \right) = 0 \tag{7}$$

Finally, we have $\nabla \cdot \mathbf{u} = 0$ since $\sum_f \alpha^f = 1$.

This derivation shows that if each fluid is incompressible, their mixture is also incompressible even though the density of the fluid mixture varies spatially.

3.3. Interface Extraction

The fluids in a group of miscible fluids are mixed together to form a fluid mixture without showing any discontinuities in physical quantities such as density and viscosity. On the other hand, a pair of different fluid groups exhibit the common interface while preserving their own physical properties. In order to cope with such discontinuities, we want to exploit existing solutions. The difficulty with this strategy is that the existing solutions depend heavily on a distance function ϕ that measures the signed distance from the interface.

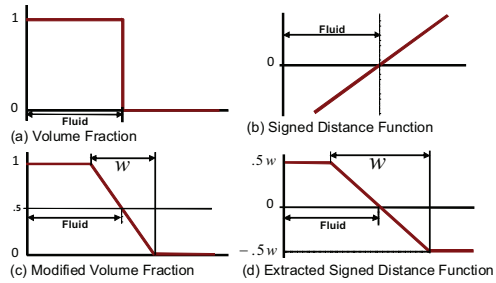

Figure 1: *volume fractions are transformed to smooth distance functions near the interface(1D Profile)*

Unlike these solutions, our approach adopts a fluid representation scheme based on volume fractions. Therefore, we modify the volume fractions in a narrow region along the interface between every pair of fluid groups to represent a distance function so that an existing solution can be employed to our problem setting.

Consider the interface between two immiscible fluids. It is embedded in a distance function ϕ, that is, the iso-contour $\phi(x) = 0$ describes the interface(Figure 1 (b)). This function changes smoothly across the interface so that differential quantities such as gradients and curvatures are well-defined. As illustrated in Figure 1 (a), the volume fraction of each fluid makes a sharp transition across the interface, which can be modeled as a Heaviside function.

$$\alpha(x) = \begin{cases} 1 & \text{if } x \text{ is a point in the region occupied by the fluid,} \\ 0 & \text{otherwise.} \end{cases}$$

We modify the volume fractions in the region near the interface to smoothly vary across the interface(Figure 1 (c)). In particular, we reset the volume fractions in the narrow region of width w along the interface by solving an Eikonal equation $||\nabla \alpha(x)|| = 1/w$ subject to constraints $0 \leq \alpha(x) \leq 1$, using a fast marching method [AS99]. After avecting all volume fractions with the BFECC method, we convert $\alpha(x)$ to a signed distant function $\phi(x)$ to accurately trace the volume fractions near the interface(Figure 1 (d)):

$$\phi(x) = w(\alpha(x) - .5). \tag{8}$$

For all of our experiments, we set $w = 6\Delta x$, where Δx is the size of a grid cell.

To handle multiple fluids, suppose that the fluids are classified into groups each being an immiscible mixture of miscible fluids. To modify the volume fractions of each group in the region near the interface, we first compute the sum of volume fractions of each group. Then we modify this value using a fast marching method. Finally, the volume fractions of member fluids are rescaled by the modified volume fraction of the group.

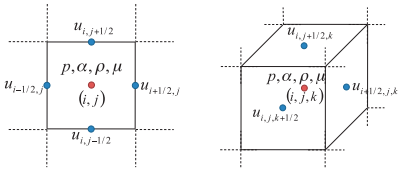

Figure 2: *2D and 3D stencil*

4. Velocity Field Computation

To solve the Navier-Stokes equations, we adopt a standard operator splitting framework [Sta99] with the fluid variables discretized on a MAC grid [HW65] as shown in Figure 2. In each iteration of simulation, we first apply advection and external forces, then project the velocity field to make it divergence free, solve for viscosity, and perform the projection step again to make sure of an incompressible velocity field [LSSF06].

For velocity advection, the BFECC scheme [KLLR07] or a semi-Lagrangian method [Sta99] is employed. However, one may use other schemes in [SSK05, KSK08, SFK*07] for accurate advection. For velocity field projection, we solve a Poisson equation with discontinuous coefficients, by adopting an existing method [LSSF06](see Section 4.1). For viscosity computation, we have to consider both variable viscosity and variable density. Thus, existing methods for variable viscosity fluid simulation [LSSF06, BB08] would not be applied directly. We gracefully get around this difficulty under the assumption that the density of each individual fluid is constant(see Section 4.2).

4.1. Velocity Field Projection

In this step, we solve the following Poisson equation for pressure computation:

$$\nabla \cdot \tilde{\mathbf{u}} - \nabla \cdot \frac{\Delta t}{\rho} \nabla p = 0 \tag{9}$$

Discretizing Equation (9) gives

$$\begin{aligned} \beta_{i+1/2} p_{i+1} \; + \; \beta_{i-1/2} p_{i-1} - \left(\beta_{i+1/2} + \beta_{i-1/2}\right) p_i \\ = \; \frac{\Delta x}{\Delta t}\left(\tilde{u}_{i+1/2} - \tilde{u}_{i-1/2}\right), \end{aligned} \tag{10}$$

where $\beta_i = \frac{1}{\rho_i}$ and $\tilde{u}$ is the intermediate velocity. For simplicity, we show only 1D discretization. The system of equations that result from Equation (10) is symmetric and positive definite, so that a preconditioned conjugate gradient(PCG) method can be employed. We update the current velocity field u^{n+1} from the previous one u^n as follows:

$$\mathbf{u}^{n+1} = \mathbf{u}^n - \frac{\Delta t}{\rho} \nabla p.$$

A difficulty in the velocity field projection is how to estimate variable coefficients β. Let G_i be the dominant group at cell i. The aggregate density ρ_i for group G_i is $(\sum_{k \in G_i} \alpha^k \rho^k)/(\sum_{k \in G_i} \alpha^k)$.

If the dominant groups at cell i and $i+1$ are the same, we take the average of the densities of cell i and $i+1$ since the density is continuous. Otherwise ($G_i \neq G_{i+1}$), the interface of the two groups, G_i and G_{i+1} passes between cell i and cell $i+1$. In this case, we adopt the discontinuous fluid methods [LFK00, LSSF06]. Thus, the coefficient $\beta_{i+1/2}$ is estimated as follows:

$$\beta_{i+1/2} = \begin{cases} \frac{2}{\rho_i + \rho_{i+1}} & \text{if } G_i = G_{i+1}, \\ \frac{\beta_i \beta_{i+1}}{(1-\theta)\beta_i + \theta \beta_{i+1}} & \text{otherwise.} \end{cases}$$

θ is defined in terms of the level set values at the adjacent cell centers,

$$\theta = \frac{|\phi(x_i)|}{|\phi(x_i)| + |\phi(x_{i+1})|},$$

where x_i is the center of cell i. In order to compute θ, we convert modified volume fractions to their respective distance functions using Equation (8).

4.2. Variable Viscosity Computation

Under the assumption that ρ is constant, the following PDE was employed for variable viscosity integration [LSSF06, BB08]:

$$\mathbf{u}_t = \frac{1}{\rho} \nabla \cdot \mu (\nabla \mathbf{u} + (\nabla \mathbf{u})^T). \tag{11}$$

The discretization of Equation (11) results in a non-symmetric system, because density ρ and viscosity μ are allowed to vary spatially in our simulation. We instead modify Equation (11) slightly so that a PCG can be applied while allowing variable density(see Appendix A).

Consequently, we have the following equation for variable viscosity integration,

$$\mathbf{u}_t = \nabla \cdot \nu (\nabla \mathbf{u} + (\nabla \mathbf{u})^T).$$

where $\nu = \sum_f \alpha^f (\mu^f / \rho^f)$. This equation can be discretized to yield a symmetric system.

The aggregate viscosity coefficient ν_i of group G_i is computed by $\nu_i = (\sum_{k \in G_i} \alpha^k \nu^k)/(\sum_{k \in G_i} \alpha^k)$, where $\nu^k = (\mu^k / \rho^k)$. Given ν_i for the dominant group G_i, $\nu_{i+1/2}$ is computed in a similar manner as $\beta_{i+1/2}$:

$$\nu_{i+1/2} = \begin{cases} \frac{\nu_i + \nu_{i+1}}{2} & \text{if } G_i = G_{i+1}, \\ \frac{\nu_i \nu_{i+1}}{(1-\theta)\nu_i + \theta \nu_{i+1}} & \text{otherwise.} \end{cases}$$

where θ is defined in the same manner as in Section 4.1.

5. Volume Fraction Advection

We combine two methods, BFECC and PLS for volume fraction advection. First, we advect every volume fraction by

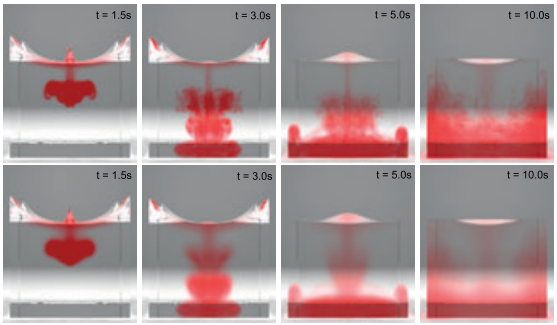

Figure 3: *Different diffusion coefficients: A small diffusion coefficient is assigned to two miscible fluids(top row). A large diffusion coefficient is assigned to the two fluids(bottom row).*

the BFECC method, given a divergence-free velocity field. This method may result in artifacts such as excessive volume loss, interface overlaps, and vacuum holes for groups each of which represents an immiscible fluid mixture. In order to alleviate these issues, we further track the interface between groups by converting the volume fractions near the interface to their respective distance functions with Equation (8), and then adopting a state-of-the-arts level set method to correct them. The corrected level set functions are converted back to the volume fractions near the interface.

Specially, for interface tracking, we employ the method by Losasso et al. [LSSF06], which is an extension of a particle level set(PLS) method [EFFM02, EMF02, ELF05] to multiple immiscible fluids. Since the volume fractions of every miscible fluid in the group are corrected using particles, each particle should convey not only the level set value of a group but also the volume fractions of the member fluids of the group. The volume fractions of particles are initially computed by linear interpolation of the volume fractions of the nearby grid points. When correcting the interface between a pair of groups using the PLS method, the volume fractions of the member fluids of each of the groups are also corrected by the volume fractions carried by the particles. After the particle correction step, the level set functions are fixed by subtracting the average of the two largest level set values in a cell to prevent the interface overlaps and vacuums. Consequently, there remain at most two immiscible fluid groups in a cell, one of which must have a volume fraction larger than or equal to 0.5.

6. Miscible Fluid Diffusion

The volume fractions of miscible fluids diffuse to each other. In order to update the volume fractions due to diffusion, we use the following governing equation:

$$\frac{\partial \alpha}{\partial t} = \nabla \cdot \mathbf{J}, \tag{12}$$

where $\mathbf{J} = D\nabla\alpha$ and D is the diffusion coefficient.

Since the diffusion flux must be zero between immiscible fluids, we set $\mathbf{J} = 0$ across the interface to prevent the diffusion between immiscible fluids. In order to effectively implement this, we exploit the notion of the dominant group of a grid cell defined in Section 3.1. We label each grid cell with its dominant group to partition the simulation domain into subregions, such that each subregion contains the grid cells with the same label(dominant group). The diffusion is done separately in each subregion. The Neumann boundary condition makes the gradient of the volume fraction vanish along the boundary. Thus, we can set the diffusion flux to zero along the boundary.

For a fluid with large diffusion coefficient, explicit numerical integration of the diffusion equation is not stable with large time steps. Therefore, we solve the diffusion equation implicitly. The implicit discretization of the diffusion equation(Equation (12)) for each subregion is shown below together with the boundary condition. For simplicity, we only show the x component of discretization:

$$\begin{gathered} -\lambda\alpha_{i-1}^{new} + (1+2\lambda)\alpha_i^{new} - \lambda\alpha_{i+1}^{new} = \alpha_i, \\ \nabla\alpha \cdot \mathbf{n} = 0 \text{ on the boundary,} \end{gathered} \tag{13}$$

where $\lambda = \frac{D\Delta t}{\Delta x^2}$, and $\mathbf{n}$ is the normal vector on the boundary. Figure 3 shows the comparison between two different diffusion coefficients.

The aggregate volume fractions near the interface should be reinitialized at every time step as diffusion smooths it out as follows: The sum of volume fractions of each group is not allowed to change although the volume fractions within the group can be changed during the diffusion. In other words, the sum of volume fractions of each group in a cell is fixed before and after the diffusion. Therefore, the volume fractions in each group are rescaled after diffusion so that their sum remains the same as before at each time step.

We further simplify diffusion exploiting the incompressibility of fluids. In general, diffusion is driven by the gradient of fluid concentration(mass fraction). We use the volume fractions instead of the mass fractions to model diffusion phenomena. This approximation makes sense since we deal with incompressible fluids. To satisfy incompressibility, the exchange of volume fractions between the neighbor grid cells must be balanced. In other words, a pair of neighbor grid cells give and take the same amount of volume fractions. From this observation, we show that the diffusion coefficients of all fluids in the same group share an equal value. Detailed derivation is available in Appendix B.

7. Visualizing Volume Fractions

We first extract the interface between fluids for visualization. We employ the marching cube scheme [LC87] to extract the 0.5 iso-surface of the aggregate fluid for each group.

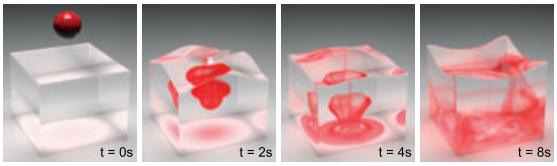

Figure 4: *Red drop falling into water*

One may use raytracing or raycasting methods to render the surface of the aggregate fluid without extracting the iso-surface [CLT07]. We then recover the volume fraction of each fluid group near the interface to represent it as a Heaviside function(Figure 1). This can be achieved by removing the artificial narrow band near the interface as follows:

$$\alpha^{new}(x) = \begin{cases} \alpha(x) & \text{if } \alpha(x) = 0 \text{ or } \alpha(x) = 1, \\ \lfloor \alpha(x) + .5 \rfloor & \text{otherwise.} \end{cases}$$

Using the recovered group volume fraction $\alpha^{new}(x)$, the volume fraction of every member in the group is rescaled to complete this task. After rendering the interface of each group of miscible fluids, we visualize the interior of the group using the recovered volume fractions of member fluids. We employ volume rendering features of PBRT [PH04] to visualize the interior of miscible fluids.

8. Results

We performed our experiments on Intel® Core2 Quad Q8400 CPU with 6GB RAM. However, we did not exploit the multi-core capability. Uniform grids were used to discretize the simulation space, and the time step was set 2 times the CFL number. In each iteration of simulation, it took about 5 to 40 seconds for solving Navier-Stokes equations, and 20 to 90 seconds for advection and diffusion. Our method performed 5 to 6 iterations per frame on average. The most time-consuming part is volume fraction correction using the particles in the advection and diffusion step. The volume fractions of each cell is represented as an N-vector where N is the number of fluids in it. Since level set values are computed on the fly whenever needed, no extra space is used to store them. For the PLS method, each particle conveys a vector of volume fractions of a group, which incurs additional space. Except this overhead, the space complexity of our method is the same as that of [LSSF06].

Multiple miscible fluid simulation: We used the following three examples to support our claim that the proposed method can handle multiple miscible fluids of different densities and viscosities, under the incompressibility assumption on each individual fluid.

In the first example, our method was used to simulate a red fluid drop falling into water in a container represented by a 100x200x100 grid. We can observe that the red drop was smoothly mixed with transparent water as shown in Figure 4. We repeated this experiment by varying fluid densities, viscosities, and diffusion coefficients. The results are available in the accompanying video.

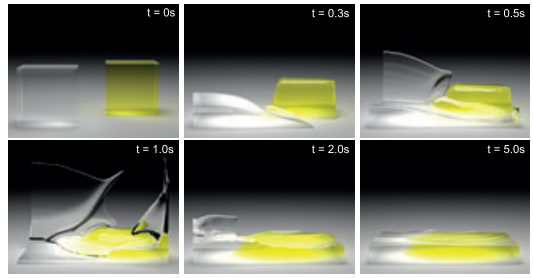

Figure 5: *Mixing honey and water*

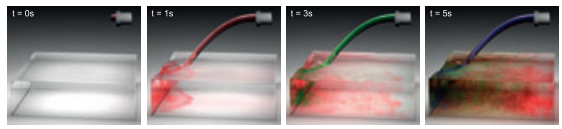

Figure 6: *Pouring three different fluids into water*

The second example shows a phenomenon of mixing honey(yellow) and water(transparent) of which the viscosities are greatly different from each other(Figure 5). Two fluid columns were initially located at the diagonally opposite corners of a 100x100x150 grid. We assigned a significantly(10000 times) higher viscosity to honey than water. Because of high viscosity contrast, the two fluids showed very different behaviors in the beginning of simulation although they were miscible with each other. After sufficient material diffusion, they behaved similarly because of the composite viscosity of their mixture.

In the last example, we employed our method to simulate three colored fluids pouring into transparent water in a 100x100x50 grid. The three fluids are colored red, blue, and green, and their densities were set as follows: $\rho_{red} > \rho_{water} > \rho_{green} > \rho_{blue}$. The four fluids are miscible with each other. Each of the three colored fluids was poured into water in turn. As shown in Figure 6, four different fluids were mixed together to result in complex color gradation inside water. This example demonstrates that our method can be used as a general tool to simulate miscible fluid flows.

Figure 9: *Rayleigh-Taylor instability*

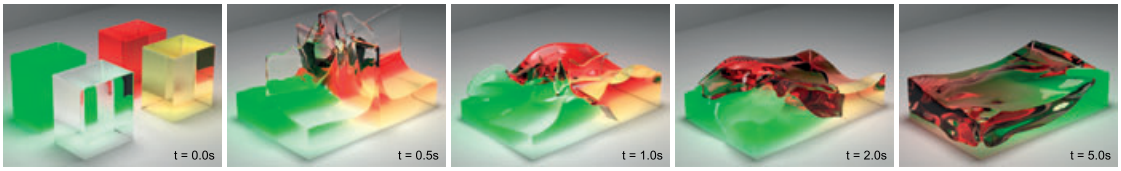

Figure 7: *Quadruple dam breaking*

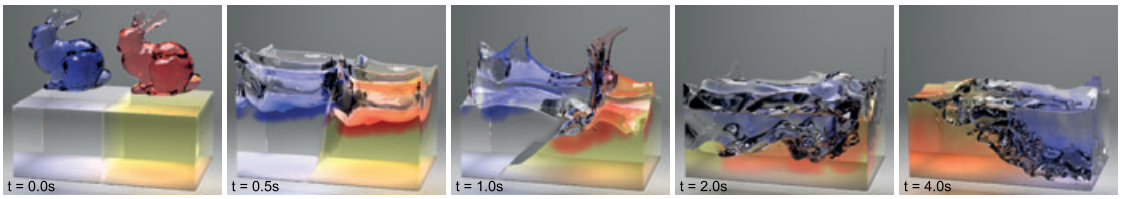

Figure 8: *Two bunny-shaped fluid chunks falling into two immiscible fluids at the bottom*

Multiple miscible and immiscible fluid simulation: Through three examples, we validate the claim that our method effectively handles multiple miscible and immiscible fluids simultaneously.

The first example shows a quadruple dam breaking scene simulated on a 100x150x150 grid. For this scene, we used four columns of fluids colored red, green, yellow, and transparent, respectively. Their densities were set as follows: $\rho_{transparent} > \rho_{green} > \rho_{red} > \rho_{yellow}$. They formed two groups of fluids, {red, yellow} and {green, transparent}. Red and yellow fluid columns were placed initially in the right side of the container. Green and transparent fluid columns were in the opposite side. As shown in Figure 7, our method allows the miscible fluids in each group to diffuse to each other while exhibiting the sharp interface between the two groups.

Our next example exhibits two bunny-shaped fluid chunks falling into two immiscible fluids at the bottom of a 100x150x150 grid. The two fluid chunks are miscible with different fluids at the bottom. The densities of four fluids were set as follows: $\rho_{red} > \rho_{yellow} > \rho_{blue} > \rho_{transparent}$. We set the diffusion coefficient between the red and the yellow fluids larger than that between the others. Accordingly, the red chunk diffused to the yellow fluid at the bottom faster than the blue chunk diffused to the transparent fluid, as shown in Figure 8.

The last example shows Rayleigh-Taylor instability with three layered fluids. The experiment was performed on a 150x150x150 grid using two groups of fluids, {blue, transparent} and {dark}. The density of the blue fluid was larger than that of the transparent fluid, which caused Rayleigh-Taylor instability between the two miscible fluids. Figure 9 shows a complex mixing phenomenon of the two miscible fluids because of the instability while keeping the discontinuous interface with the dark fluid.

9. Discussion

The diffusion normalization(see Section 6) may lead to mass changes for individual fluids. For a cell distant from the interface, the sum of volume fractions is one before and after the diffusion. Therefore, the diffusion normalization does not affect the volume fractions in such a cell. However, for a cell near the interface, the volume fractions are modified to result in mass changes after the diffusion normalization since their sum is not equal to one. The effect of the mass changes is not visually noticeable because it occurs only the narrow band near the interface. In our experiments, the mass changes due to the diffusion normalization are less than 0.01% even for the rather large diffusion coefficient.

In real world, the volume of the mixtures of miscible fluids tends to be smaller than the sum of their individual fluid volumes because of the different sizes of fluids molecules. This is similar to what happens when mixing sand and rocks. This phenomena could be taken care of by incorporating a microscopic scheme that can handle the volume of a mixture of miscible fluids explicitly beyond the diffusion. We leave it as a future research topic.

Although we assume that the groups of miscible fluids are disjoint, this assumption may not always hold true. For example, consider three fluids, water, oil and liquid soap. Water and oil are not miscible with each other. However, each of these is miscible with liquid soap. Thus, it is not possible to partition the fluids into disjoint groups in such a case. We also leave this as a future research topic.

In our Rayleigh-Taylor instability example(Figure 9), it is hard to see the details of fluid features because of the sparse resolution of the simulation domain. Incorporating an adaptive grid into our framework is yet another interesting research venue for capturing fine-scale detail of fluid-fluid interaction.

10. Conclusion

In this paper, we present a hybrid approach to simulating a multiple fluid flow including both miscible and immiscible fluids. Providing a conversion scheme between volume fractions and level set functions, we take advantage of both. We adopt volume fractions as the main representation scheme of fluids for simulation, while transforming these near the interface into(or back from) their respective level set functions, if necessary, to employ existing solutions. From the technical point of view, our main contributions are to provide cornerstones for multiple fluid simulation with variable density and variable viscosity: in particular, incompressibility condition enforcement, variable density and viscosity handling, combining volume fractions with distance functions, and simplification of material diffusion.

Our method is based on the standard operator-splitting method unlike the LBM-based approaches, so that it can be easily integrated into the conventional fluid simulation pipeline. We believe that dynamic solid objects may also be simulated within our framework by incorporating the solid-fluid coupling method of [BBB07].

Acknowledgements

We would like to thank Jihyeon Yi and Donghoon Sagong for their help. This work was supported by the Korea Science and Engineering Foundation(KOSEF) grant funded by the Korea government(MEST) (No. 2009-0058607).

References

[AGDJ08] ANDERSON J. C., GARTH C., DUCHAINEAU M. A., JOY K. I.: Discrete multi-material interface reconstruction for volume fraction data. *Computer Graphics Forum 27*, 3 (2008), 1015–1022. 3

[AMW98] ANDERSON D. M., MCFADDEN G. B., WHEELER A. A.: Diffuse-Interface Methods in Fluid Mechanics. *Annual Review of Fluid Mechanics 30* (1998), 139–165. 3

[AS99] ADALSTEINSSON D., SETHIAN J. A.: The fast construction of extension velocities in level set methods. *Journal of Computational Physics 148*, 1 (1999), 2 – 22. 4

[BB08] BATTY C., BRIDSON R.: Accurate viscous free surfaces for buckling, coiling, and rotating liquids. In *Proceedings of the 2008 ACM/Eurographics Symposium on Computer Animation* (July 2008), pp. 219–228. 2, 5

[BBB07] BATTY C., BERTAILS F., BRIDSON R.: A fast variational framework for accurate solid-fluid coupling. *ACM Trans. Graph. 26*, 3 (2007), 100. 9

[CD98] CHEN S., DOOLEN G. D.: Lattice boltzmann method for fluid flows. *Annual Review of Fluid Mechanics 30*, 1 (1998), 329–364. 2

[CLT07] CRANE K., LLAMAS I., TARIQ S.: Real-time simulation and rendering of 3d fluids. *GPU Gems 3 Chapter 30* (2007). 7

[EFFM02] ENRIGHT D., FEDKIW R., FERZIGER J., MITCHELL I.: A hybrid particle level set method for improved interface capturing. *J. Comput. Phys. 183*, 1 (2002), 83–116. 2, 6

[ELF05] ENRIGHT D., LOSASSO F., FEDKIW R.: A fast and accurate semi-lagrangian particle level set method. *Computers and Structures 83* (2005), 479–490. 2, 6

[EMF02] ENRIGHT D., MARSCHNER S., FEDKIW R.: Animation and rendering of complex water surfaces. *ACM Trans. Graph. 21*, 3 (2002), 736–744. 2, 6

[GA08] GAUDLITZ D., ADAMS N. A.: On improving mass-conservation properties of the hybrid particle-level-set method. *Computers & Fluids 37*, 10 (2008), 1320 – 1331. 3

[GDSS05] GARIMELLA R. V., DYADECHKO V., SWARTZ B. K., SHASHKOV M. J.: Interface reconstruction in multi-fluid, multi-phase flow simulations. In *In Proc. of International Meshing Roundtable* (September 2005), pp. 19–32. 1, 3

[HK05] HONG J.-M., KIM C.-H.: Discontinuous fluids. *ACM Trans. Graph. 24*, 3 (2005), 915–920. 2

[HN81] HIRT C. W., NICHOLS B. D.: Volume of fluid (vof) method for the dynamics of free boundaries. *Journal of Computational Physics 39*, 1 (1981), 201 – 225. 1, 2, 3

[HW65] HARLOW F. H., WELCH J. E.: Numerical calculation of time-dependent viscous incompressible flow of fluid with free surface. *Physics of Fluids 8*, 12 (1965), 2182–2189. 1, 5

[KFL00] KANG M., FEDKIW R. P., LIU X.-D.: A boundary condition capturing method for multiphase incompressible flow. *J. Sci. Comput. 15*, 3 (2000), 323–360. 2

[KLLR07] KIM B., LIU Y., LLAMAS I., ROSSIGNAC J.: Advections with significantly reduced dissipation and diffusion. *IEEE Transactions on Visualization and Computer Graphics 13*, 1 (2007), 135–144. 2, 5

[KSK08] KIM D., SONG O.-Y., KO H.-S.: A semi-lagrangian cip fluid solver without dimensional splitting. *Computer Graphics Forum 27*, 2 (April 2008), 467–475. 5

[LC87] LORENSEN W. E., CLINE H. E.: Marching cubes: A high resolution 3d surface construction algorithm. *SIGGRAPH Comput. Graph. 21*, 4 (1987), 163–169. 6

[LFK00] LIU X.-D., FEDKIW R. P., KANG M.: A boundary condition capturing method for poisson's equation on irregular domains. *J. Comput. Phys. 160*, 1 (2000), 151–178. 2, 5

[LSSF06] LOSASSO F., SHINAR T., SELLE A., FEDKIW R.: Multiple interacting liquids. *ACM Trans. Graph. 25*, 3 (2006), 812–819. 1, 2, 3, 5, 6, 7

[MCG03] MÜLLER M., CHARYPAR D., GROSS M.: Particle-based fluid simulation for interactive applications. In *SCA '03: Proceedings of the 2003 ACM SIGGRAPH/Eurographics symposium on Computer animation* (Aire-la-Ville, Switzerland, Switzerland, 2003), Eurographics Association, pp. 154–159. 2

[MMTD07] MULLEN P., MCKENZIE A., TONG Y., DESBRUN M.: A variational approach to eulerian geometry processing. *ACM Trans. Graph. 26*, 3 (2007), 66. 2

[Mon05] MONAGHAN J.: Smoothed particle hydrodynamics. *Reports on Progress in Physics 68* (2005), 1703–1759(57). 2

[MSKG05] MÜLLER M., SOLENTHALER B., KEISER R., GROSS M.: Particle-based fluid-fluid interaction. In *SCA '05: Proceedings of the 2005 ACM SIGGRAPH/Eurographics symposium on Computer animation* (New York, NY, USA, 2005), ACM, pp. 237–244. 1, 2

[MUM*06] MIHALEF V., UNLUSU B., METAXAS D., SUSSMAN M., HUSSAINI M. Y.: Physics based boiling simulation. 317–324. 3

[OS88] OSHER S., SETHIAN J. A.: Fronts propagating with curvature dependent speed: algorithms based on hamilton-jacobi formulations. *Journal of Computational Physics 79* (1988), 12–49. 1

[PH04] PHARR M., HUMPHREYS G.: *Physically Based Rendering: From Theory to Implementation*. Morgan Kaufmann, 2004. 7

[PKW*08] PARK J., KIM Y., WI D., KANG N., SHIN S. Y., NOH J.: A unified handling of immiscible and miscible fluids. *Computer Animation and Virtual Worlds 19*, 3-4 (2008), 455–467. 1, 2, 3, 4

[PP04] PILLIOD JR. J. E., PUCKETT E. G.: Second-order accurate volume-of-fluid algorithms for tracking material interfaces. *J. Comput. Phys. 199*, 2 (2004), 465–502. 3

[PTB*03] PREMOZE S., TASDIZEN T., BIGLER J., LEFOHN A., WHITAKER R. T.: Particle-based simulation of fluids. *Computer Graphics Forum 22* (2003), 401–410(10). 2

[SFK*07] SELLE A., FEDKIW R., KIM B., LIU Y., ROSSIGNAC J.: An unconditionally stable maccormack method. *J. Comput. Phys. (in review)* (2007). 5

[SP00] SUSSMAN M., PUCKETT E. G.: A coupled level set and volume-of-fluid method for computing 3d and axisymmetric incompressible two-phase flows. *Journal of Computational Physics 162*, 2 (2000), 301 – 337. 3

[SSK05] SONG O.-Y., SHIN H., KO H.-S.: Stable but nondissipative water. *ACM Trans. Graph. 24*, 1 (2005), 81–97. 5

[Sta99] STAM J.: Stable fluids. In *SIGGRAPH '99: Proceedings of the 26th annual conference on Computer graphics and interactive techniques* (New York, NY, USA, 1999), ACM Press/Addison-Wesley Publishing Co., pp. 121–128. 1, 2, 4, 5

[Sus03] SUSSMAN M.: A second order coupled level set and volume-of-fluid method for computing growth and collapse of vapor bubbles. *Journal of Computational Physics 187*, 1 (2003), 110 – 136. 3

[WYS08] WANG Z., YANG J., STERN F.: Comparison of particle level set and clsvof methods for interfacial flows. 46th Aerospace Sciences Meeting and Exhibit, American Institute of Aeronautics and Astronautics. 3

[You82] YOUNGS D.: Time-dependent multimaterial flow with large fluid distortion. *K. Morton, M. Baines (Eds.), Numerical Methods for Fluid Dynamics, Academic Press, New York,* (1982), 273–285. 3

[YZF07] YUE P., ZHOU C., FENG J. J.: Spontaneous shrinkage of drops and mass conservation in phase-field simulations. *Journal of Computational Physics 223*, 1 (10 April 2007), 1–9. 3

[ZBWL07] ZHU H., BAO K., WU E., LIU X.: Stable and efficient miscible liquid-liquid interactions. In *VRST '07: Proceedings of the 2007 ACM symposium on Virtual reality software and technology* (New York, NY, USA, 2007), ACM, pp. 55–64. 1, 2, 4

[ZLLW06] ZHU H., LIU X., LIU Y., WU E.: Simulation of miscible binary mixtures based on lattice boltzmann method. *Computer Animation and Virtual Worlds 17*, 3-4 (2006), 403–410. 1, 2, 4

Appendix A: Viscosity Derivation

Based on the operator splitting framework, viscosity can be integrated by solving the following PDE:

$$\mathbf{u}_t = \frac{1}{\rho}\nabla\cdot\tau, \text{ or } \rho\mathbf{u}_t = \nabla\cdot\tau,$$

where $\tau = \mu(\nabla\mathbf{u} + (\nabla\mathbf{u})^T)$.

For each fluid f, we have

$$\rho^f\mathbf{u}_t = \nabla\cdot\tau^f,$$

where $\tau^f = \mu^f(\nabla\mathbf{u} + (\nabla\mathbf{u})^T)$.

This equation, when integrated over a cell gives

$$\alpha^f\int_c \rho^f\mathbf{u}_t dV = \alpha^f\int_c \nabla\cdot\tau^f dV.$$

Since volume fraction α^f is assumed to be constant within a cell,

$$\alpha^f\int_c \rho^f\mathbf{u}_t dV = \int_c \alpha^f\rho^f\mathbf{u}_t dV.$$

From the divergence theorem,

$$\alpha^f\int_c \nabla\cdot\tau^f dV = \alpha^f\int_{\partial c}\tau^f d\mathbf{S} = \int_{\partial c}\alpha^f\tau^f d\mathbf{S} = \int_c \nabla\cdot(\alpha^f\tau^f)dV.$$

Therefore,

$$\alpha^f\rho^f\mathbf{u}_t = \nabla\cdot(\alpha^f\tau^f).$$

Dividing both sides by ρ^f,

$$\alpha^f\mathbf{u}_t = \nabla\cdot(\alpha^f\tau^f/\rho^f).$$

Here, we make use of the assumption that ρ^f is constant for all f. Summing these equations over all fluids in a cell,

$$\sum\alpha^f\mathbf{u}_t = \nabla\cdot\sum(\alpha^f\tau^f/\rho^f)$$

which is simplified to

$$\mathbf{u}_t = \nabla\cdot\nu(\nabla\mathbf{u} + (\nabla\mathbf{u})^T),$$

where

$$\nu = \sum\alpha^f(\mu^f/\rho^f).$$

Appendix B: Diffusion Coefficients

Let two miscible fluids, A and B be in cells i and $i+1$, respectively. The diffusion fluxes for fluids A and B are given as follows

$$\mathbf{J}^A_{right} = D^A\frac{\alpha^A_{i+1} - \alpha^A_i}{\Delta x}$$
$$\mathbf{J}^B_{left} = D^B\frac{\alpha^B_{i+1} - \alpha^B_i}{\Delta x},$$

where $\mathbf{J}^A_{right}$ and $\mathbf{J}^B_{left}$ are the diffusion fluxes for fluid A and B, respectively. Since the exchange of flux between two cells is balanced, we set the sum of the diffusion fluxes zero,

$$D^A\frac{\alpha^A_{i+1} - \alpha^A_i}{\Delta x} + D^B\frac{\alpha^B_{i+1} - \alpha^B_i}{\Delta x} = 0.$$

Therefore,

$$D^A\left(\alpha^A_{i+1} - \alpha^A_i\right) + D^B\left(\alpha^B_{i+1} - \alpha^B_i\right) = 0.$$

Since $\alpha^B = 1 - \alpha^A$,

$$\left(D^A - D^B\right)\alpha^A_{i+1} + \left(D^A - D^B\right)\alpha^A_i = 0.$$

Since above equality is satisfies for arbitrary α^A, we have $D^A = D^B$. This also holds true for more than three miscible fluids.